13th International Conference on
Structural Health Monitoring of Intelligent Infrastructure
DOI: 10.3217/978-3-99161-057-1-140

Preliminary results from a field application of dynamic monitoring on three spans of a railway bridge

Eleonora Massarelli[1, 0009-0001-5172-0804], Marco Civera[1, 0000-0003-0414-7440], Giulio Ventura[1, 0000-0001-5464-6091], Bernardino Chiaia[1, 0000-0002-5469-2271]

[1]Politecnico di Torino, Department of Structural, Geotechnical and Building Engineering (DISEG), Corso Duca degli Abruzzi 24, 10129 Turin, Italy

email: marco.civera@polito.it

ABSTRACT: Vibration-based Structural Health Monitoring is of the foremost importance for critical civil infrastructures, especially concerning the safety of the train transport network. In fact, even minor structural changes might cause derailment and potentially fatal accidents. This contribution reports some preliminary analyses carried out on 52 accelerometric recordings collected over two consecutive days from three spans of a railroad bridge. The acquisitions include several train passages and the quiet periods between them, when the structure was excited only by ambient vibrations (i.e. random microtremors), thus allowing Ambient Vibration Testing (AVT). Specifically, a newly developed Automated Operational Modal Analysis (AOMA) algorithm was applied. Its results are here compared to state-of-the-art commercial software (ARTeMIS). Some considerations regarding the effects of train passages are also briefly reported, as well as directions for current and future research work in this field.

KEYWORDS: automated operational modal analysis, railway bridge, structural health monitoring, operational modal analysis, vibration-based monitoring

1 INTRODUCTION

Railways are an essential component of civil infrastructures, representing one of the most critical parts of national and transnational transportation and communication systems. In particular, railway bridges are a crucial element in this context. Being affected by degradation processes of various natures and durations, they constitute the most vulnerable elements for the safety of the whole railway infrastructure, with potential consequences for the safety of goods and people.

In fact, considering that different parts of every railway infrastructure are connected from the superstructure, i.e. the ballast and the rails, even minor structural changes without complete structural failure might cause derailment and potentially fatal accidents.

For all these reasons, a robust understanding and awareness of the daily operations and safety concerns is required, given that many passengers use railway lines daily. In Europe, 35% of the more than 300,000 railway bridges, which are distributed over a total of 200,000 km of railways, exceed 100 years of operational life [1]. In particular, in Italy, the majority of railway viaducts built between the 1950s and 1970s consist of prestressed concrete bridges (PRC); hence, special attention should be granted to these ageing infrastructures [2].

Railway bridges are exposed to several factors which cause degradation. These include harsh environmental conditions, significant live loads – mainly due to the increase of traffic loads in the last decades, including high-speed trains – material ageing, and other rare or extreme events (i.e. impacts from accidents, earthquakes, etc.). Other than material ageing, PRC bridges are subjected to damages due to: corrosion of normal reinforcement steel bars as well as prestressing tendons; prestressing losses; construction errors (incorrect grouting of tendons ducts, for example); and many other potential natural or human-made hazards [3]. Inadequate maintenance is also a practice that could result in further damages, often non-recoverable. Finally, hidden grouting defects of prestressing sheaths can lead to corrosion, reducing the area of prestressing steel with consequent bearing capacity decrease.

As a result, all these factors contribute to the potential development and growth of structural damage over time.

Per established tradition, visual inspection still plays an essential role in identifying superficial defects and evaluating the overall condition of the examined structure. However, visual inspections are labour-intensive, time-consuming, and often rely on the operator's experience level, which significantly impacts the accuracy, objectiveness, and reliability of structural condition evaluations.

Hence, the application of automated and objective anomaly detection is fundamental. This is the paradigm of Structural Health Monitoring (SHM) solutions [4]; their application to railway bridges is important to maintain operational safety, expand the structure's lifespan, and reduce maintenance costs. In particular, Vibration-Based SHM, which relies on analysing the vibrational response of structures to identify damage indicators, is one of the most used techniques to identify and monitor changes in the dynamic properties of a structure. In this framework, to identify such pathologies, the first step involves extracting the target structure's damage-sensitive features (DSFs) from the monitoring data – that is, natural frequencies, damping ratios, and associated mode shapes from acceleration time series. Possible changes in modal parameters over time could be a manifestation of both global and local damages.

DOI: 10.3217/978-3-99161-057-1-140

In particular, natural frequencies are mainly sensitive to global damages and structural modifications. However, the global stiffness of a structure is often influenced by variations in normal environmental factors, such as temperature, and their influence (daily or seasonal gradients) can be significant enough to mask the presence of certain damages. Notably, local damage up to moderate severity has a minor influence on eigenfrequencies. On the other hand, mode shapes are more sensitive to local damages than natural frequencies and less sensitive to temperature variations [5], [6]. The main disadvantage is that a dense sensor grid is required to ensure effective damage localisation, a choice which is generally costly when conventional sensors, such as accelerometers, are employed.

Nevertheless, in both mode shape-based and natural frequency-based SHM, the key point is to extract high-quality modal parameters from the recorded time series; henceforth, accurate identifications are strictly required.

This short contribution presents the results of a novel output-only System Identification (SI) algorithm, applied to an experimental test campaign on a prestressed reinforced concrete railway bridge. In this context, the present study focuses on analysing the recorded accelerometric monitoring data of the viaduct's deck.

The case study presented here has been equipped with highly sensitive accelerometers on three spans, collecting data for two consecutive days. The acquired acceleration data are processed using the proposed Automated Operational Modal Analysis (AOMA) approach based on the SSI-COV algorithm [7] using a code developed in MATLAB environment. Dynamic identifications obtained considering ambient vibrations provide repeatable and directly comparable results between identical spans. Furthermore, as a benchmark, the results are compared to the ones obtained with the commercial software (ARTeMIS).

The remainder of this paper is organised as follows. Section 2 describes the structure, the dynamic monitoring system and the data acquired. In Section 3, the Automated Operational Modal Analysis procedure for dynamic monitoring is briefly described. The results obtained considering the environmental excitation of the structure are then reported in Section 4, followed by the analyses repeated with the commercial software ARTeMIS; such results are then compared. Finally, the conclusions of the study carried out for this structure follow in Section 5.

2 EXPERIMENTAL TEST CAMPAIGN

2.1 Description of the structure

The railway viaduct under investigation consists of 46 spans, each equal to 20 m, for a total length of 920 m. The individual spans are characterised by a simply supported static scheme and consist of eight prestressed concrete girders with I cross-sections, connected by a 20 cm thick upper slab, and four transversal beams having rectangular cross-sections. The main beams are 1.40 m high and have 1.20 m spacing, such that, considering the two lateral cantilever slabs supporting the parapets, the total width of the deck is approximately 12.40 m, allowing the support of two train tracks (see Figure 1 and Figure 2). The beams' prestressing reinforcement is arranged in the lower flange and, according to the original design drawings, consists of a total of 29 cables arranged in 3 rows, sheathed in ducts at the supports. As mentioned, PRC beams are widely used in railway bridges, where dynamic loads from passing trains demand high stiffness and serviceability. The prestressing process introduces compressive forces into the concrete; these forces counteract tensile stresses, preventing cracking and the resulting stiffness reduction. This, compared to a beam of equivalent size in conventional (non-prestressed) RC, results in lower deflections under load and allows for larger spans. At the same time, lower amplitude vibrations are generated under working conditions, which is useful for safety and comfort in operating conditions but makes AVT and output-only identifications more challenging, requiring high-quality accelerometers.

Figure 1: View of a typical span of the railway viaduct.

The standard pier has a pseudo-rectangular reinforced concrete geometry (maximum dimensions 11.0 x 1.50 m). The 45 piers range from a minimum height of 2.5 m to a maximum of 5 m along the longitudinal direction. The foundation of the piers consists of a RC plinth lying on deep foundations (i.e. piles).

Figure 2: Intrados view of a typical span of the case study with the PRC beams.

DOI: 10.3217/978-3-99161-057-1-140

2.2 *Structural health monitoring (SHM) system*

Because of the extension of the viaduct and its static scheme, with simply supported and nominally equal spans, only a part of the entire structure has been investigated. Specifically, three spans have been instrumented. Four uniaxial accelerometers were installed for each span under study in the positions showed in Figure 3 and with the numbering indicated. Measurements of only the vertical acceleration components were acquired for two consecutive days. This placement aimed to associate the obtained frequencies with both vertical and torsional vibrational modes.

Due to the high stiffness of prestressed reinforced concrete railway bridges, accelerometers with high sensitivity and low background noise are required. In the present case, PCB piezoelectric accelerometers model 393B12 were used, with a sensitivity of 10 V/g and a noise of 0.32 $\mu g/\sqrt{Hz}$ on the 10 Hz band.

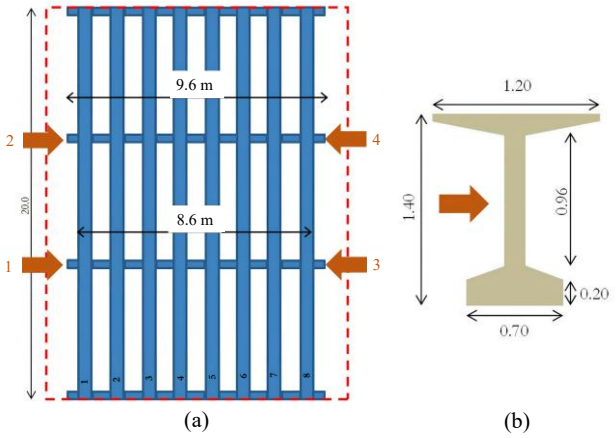

Figure 3: Scheme of the typical span (a) and position of the accelerometers on the main beams near the cross beams (b). The numbers in red (1 to 4) indicate the different output channels.

The instrumentation configuration differs between the spans as follows:

- in one span, the four accelerometers were installed at the end of the cross beams (transverse distance 9.6 m).
- in the other two spans, the four accelerometers were installed on the web of the main beams in proximity of the cross beams (transverse distance 8.6 m, see Figure 3 (b).

The experimental tests were designed to identify the bridge's modal parameters and verify the structure's response under normal operating conditions. For this reason, some signals would inevitably contain train passages alongside ambient vibrations. 20 recordings were acquired for the first span; 16 other recordings were taken for the other two spans, referred to as numbers 2 and 3. All acquisitions were made with a sampling frequency f_s = 100 Hz and a 24-bit acquisition system. That provides a wide margin with respect to the highest natural frequency of interest (16 Hz, as will be shown in the following Sections, thus well below the Nyquist limit $f_s/2$ = 50 Hz). The duration of each measurement was about 15 minutes. Examples of recorded time series of the raw acceleration data for one of the instrumented spans, showing all acquisition channels, are displayed in Figure 4.

The vertical acceleration signals acquired by the four acquisition channels for each instrumented span were analysed after the cleaning and pre-processing phase. In particular, after identifying the signals containing train passages, the corresponding signal portions were isolated and saved separately. The remaining parts, thus corresponding to ambient excitation, were likewise isolated, stored separately, and analysed in the subsequent steps. In this way, 80 signals were obtained, of which only those of appropriate length (> 4 minutes) were used for the successive identification steps. The signal duration was found to be consistent with the range recommended in [8] for accurate damping estimation, i.e. 1000-2000 times the natural period of the first mode (2 to 4 minutes in the present case study), thus reliable results are ensured even when signals are segmented.

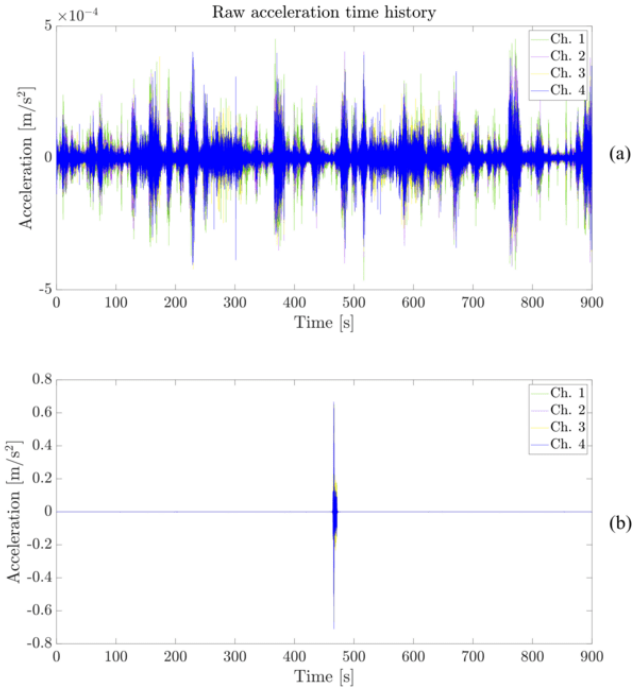

Figure 4: Example of a signal acquired in one of the spans under ambient vibration conditions (a) and with a passing train (b) after the pre-processing.

3 AUTOMATED OPERATIONAL MODAL ANALYSIS (AOMA) FOR SHM

The objective of any Automated Operational Modal Analysis (AOMA) procedure is the extraction of modal parameters through the analysis of vibration measurements. The procedure is a multi-stage process that involves several sequential steps. It begins with data pre-processing and the choice of the optimal algorithm parameters, followed by the system identification phase, then the sifting of the identified modal parameters, and finally, the estimation of cluster-wide values and their validation, as well-documented in [9] and [10]. In this context, the core of the procedure, i.e. the system identification phase, is carried out by applying the Stochastic Subspace Identification (SSI) method, which is a popular parametric time

DOI: 10.3217/978-3-99161-057-1-140

domain algorithm based on state-space identification [7]. Several authors have proposed AOMA procedures to try to address the aspect of automating the interpretation of the stabilisation diagram and the following extraction of the physically meaningful modes of the structure [8], [11], [12].

3.1 AOMA algorithm and modal parameters' selection

In the present study, the dynamic identification of the structure decks was performed using the well-known SSI (Stochastic Subspace Identification) Operational Modal Analysis algorithm with clustering analysis (DBSCAN - Density-Based Spatial Clustering of Applications with Noise) to facilitate the identification of actual vibration modes [13], [14].

SSI returns all identified modal parameters, which are generally represented in a stabilisation diagram, which is a visual tool used to facilitate the interpretation of results showing the poles (modes) characterised by the natural frequencies, damping ratios, and eigenvectors identified in relation to the order of the dynamic system chosen a priori. However, these identified poles include the physical modes as well as many spurious modes; the latter ones, which are due to measurement noise misidentified as vibration modes, need to be disregarded to identify only valid results correctly. In the stabilisation diagram, poles aligned in a vertical line are stable as the model order changes and, therefore, are deemed to represent a physical mode. The automatic cleaning and interpretation phase of the stabilisation diagram consists of defining a set of criteria to distinguish physical poles from spurious and mathematical ones. The steps enabling this procedure are briefly outlined below:

- hard validation criteria (HVC), consisting of the elimination of poles with negative or excessively high damping ratios (> 20%) and those with eigenvectors not coming in complex conjugate pairs;
- soft validation criteria (SVC), concerning the introduction of comparison parameters between the modal parameters of the different poles (hence the distance in the stabilisation diagram) and elimination of those that do not fall within the selected thresholds, following the work done by Mugnaini et al. [15];
- application of the DBSCAN algorithm to group the poles with similar modal characteristics and discard any other outlier poles according to parameters that vary for each dataset. Each identified cluster individuates a set of probable physical modes; therefore, the modal parameters representative of an entire cluster are estimated as the average of the cluster values f_m, ξ_m [10].

Determining the corresponding mode shape is essential to discern the modes with actual physical significance.

3.2 ARTeMIS software

The commercial dynamic identification software ARTeMIS was used as a benchmark to validate the results obtained from the developed AOMA code. ARTeMIS is a powerful operational and experimental modal analysis software. The results are obtained through a Data-Driven Stochastic Subspace Identification algorithm implementation.

4 DISCUSSION OF RESULTS

4.1 AOMA results

SSI needs the definition of two fundamental parameters:

- the range of model order, going from n_{min}= 20 to n_{max} = 130,
- the number of block rows of the Hankel matrix, defined as $f_s/2$ [7].

For a fair comparison, these parameters were set once and kept untouched for all analyses (all signal tracts of all spans). The comparison parameters for the stabilisation diagram [13] reported above are set equal to:

- $df < 0.005$
- $0 < d\xi < 10$ %
- (1 - MAC) < 0.05

Figure 5 shows a 'cleaned' stabilisation diagram at the end of the clustering phase (in fact it can be seen how each cluster is identified by a different colour), taken by one example of one of the instrumented spans. In this particular case, the frequency range of interest goes from 8 to 20 Hz, where clear peaks can be observed. In the same way, a diagram of the damping ratios versus natural frequencies is represented in Figure 6. The identified clusters are linked to the ones in Figure 5, i.e. displayed with the same colours.

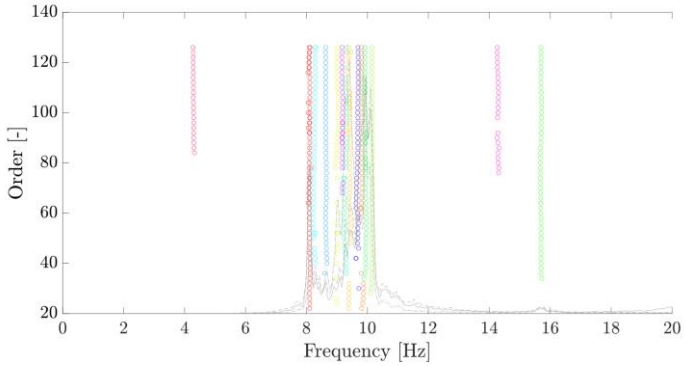

Figure 5: Example of stabilisation diagram with identified clusters.

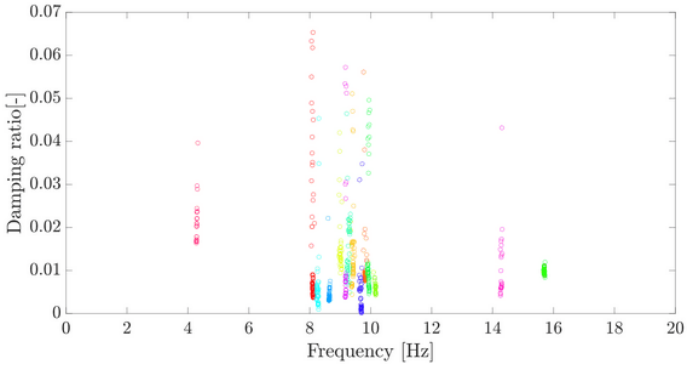

Figure 6: Example of frequencies vs damping ratios diagram with identified clusters.

Finally, Figure 7 shows the occurrence of the values of identified natural frequencies for the deck of one of the instrumented spans, considering all the ambient vibration signals used.

DOI: 10.3217/978-3-99161-057-1-140

By comparing all the results obtained from the different signals, the natural frequencies with the highest occurrence and corresponding to mode shapes with physical significance were identified. The following figure (Figure 8) shows the experimental vibration modes of the structure, with distribution diagrams of the natural frequencies and an axonometric view of the mode shapes with an indication of measurement points for each identified mode.

Concerning the 2nd mode, it is noteworthy to point out the fact that it has been identified twice. Although the identified mode shape seems to indicate that it is the same mode, there is no certainty as to the exact corresponding frequency. One could conservatively assume that one of the two estimated modes corresponds to some residual effects of a lateral mode. Still, since all output channels are vertical, the algorithm can only extract the mode shape of the closest mode with vertical components, i.e., the first torsional. Here and for the rest of the article, these are referred to as modes '2a' and '2b'. Instead, the 1st mode can be identified as the first flexural mode of the deck.

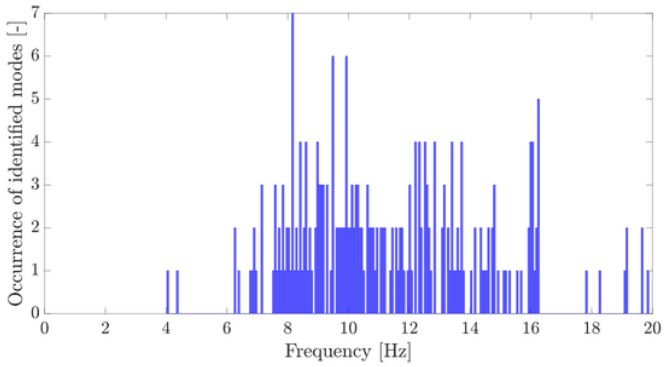

Figure 7: Histogram representing the occurrence of natural frequency estimates of probable physical vibration modes.

For the mode identified as 'mode 3' in Figure 8, given the positioning and limited number of sensors, the corresponding mode shape is similar to the first flexural one. It could be assumed that the mode in question is instead related to a local mode of the deck, whose shape could only be detected with a denser sensor network. However, it should be noted that for the practical purposes of detecting damage structural phenomena for this type of structure, the first two modes are generally significant, as they are also identifiable with greater accuracy and repeatability. The estimated damping ratios are around 2 % for most identifications, except for mode 3, for which it is about 1 %.

Table 1 shows the values of the identified natural frequencies for each span. The first torsional mode identified twice with different frequencies is reported as 'mode 2a' and 'mode 2b'. Furthermore, the low standard deviation values confirm that the three instrumented spans, nominally identical, are very similar in terms of dynamic response (and thus mechanical properties). This suggests that any damage in one of them would be easily detected not only by comparing the historical and current response of the span in question but also by comparing it with the other spans contemporaneously monitored – i.e. a sort of population-based SHM [16]. Indeed, this approach falls into the concept of population-based SHM.

Table 1: Summary of the natural frequencies identified by the MATLAB code (all values in Hz) for the relevant modes in the three instrumented spans, with average and standard deviation values (St.Dev).

	Mode 1	Mode 2a	Mode 2b	Mode 3
Span 1	8.148	9.205	10.084	15.873
Span 2	8.117	9.181	10.112	16.020
Span 3	8.126	9.142	10.123	15.907
Average	**8.130**	**9.176**	**10.106**	**15.933**
St.Dev	**0.016**	**0.032**	**0.020**	**0.077**

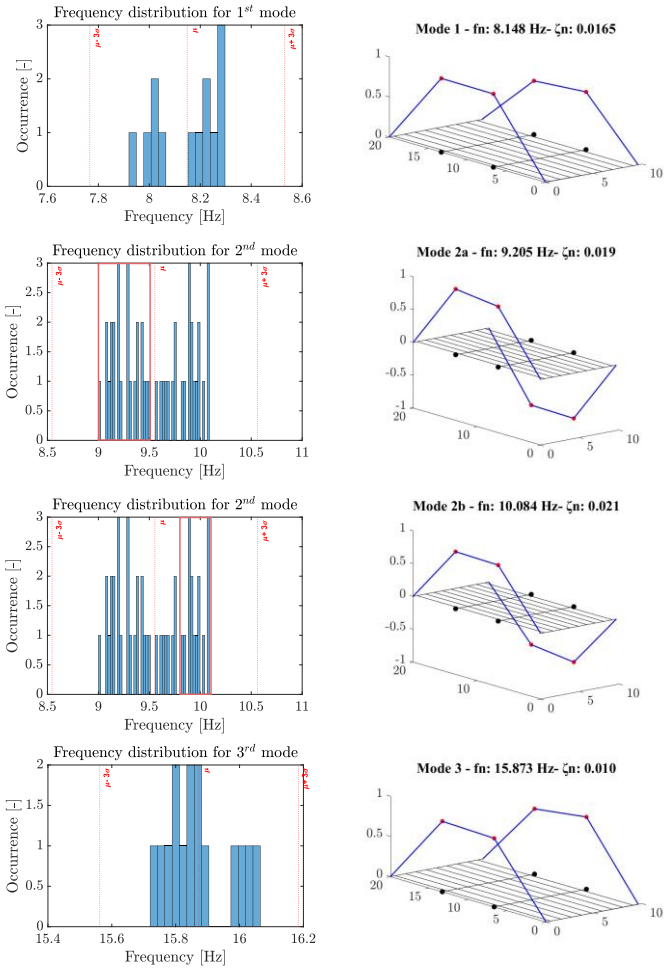

Figure 8: Distribution diagram of the identified natural frequencies and axonometric view of the identified mode shapes with an indication of the measurement points in red for mode 1 (a), modes 2a (b), and 2b (c), and local mode 3 (d).

Notably, the first mode shape was found to be slightly asymmetric, with the vibrations on one side ~20% larger than the other. This behaviour was confirmed in all acquisitions with both the MATLAB code and ARTeMIS (see next Section). Conversely, the other three mode shapes behave very symmetrically, with differences <4% between the two sides.

4.2 ARTeMIS results comparison

The results from the ARTeMIS software were obtained by importing, via a .cfg text file, the geometric model of the

DOI: 10.3217/978-3-99161-057-1-140

individual deck and the information regarding the actual position of the sensors, which was the same for the three instrumented spans. The acceleration time histories used are those from the pre-processing phase described in Section 2.2 and relative to ambient vibrations. The results showed in this section refer to a single example file belonging to one of the instrumented decks, but the overall outputs, analysed manually, are in line with those of the other acquisitions on the same span and the others. All results refer to the analysis with ambient noise, i.e. eliminating train passages.

At first, Frequency Domain Decomposition (FDD) was used, a frequency domain features extraction technique with manual peak selection to perform a preliminary analysis; the results obtained with this method are shown in Figure 9 on the left side. All natural frequency values estimated for the first three modes are very similar to those verified by MATLAB code on the entire dataset of available signals. As already observed through the AOMA code, there is a substantial similarity between the first and third modes. Moreover, as better detailed below, for each span, just one of the two modes named as 'mode 2' can be estimated by applying FDD.

Stochastic Subspace Identification with Unweighted Principal Component (SSI-UPC) [7] was then used. Regarding the definition of the SSI parameters, the same model order range as selected in the MATLAB code, i.e. from n_{min} = 20 to n_{max} = 130, was set for direct comparability. Relative to the same example presented and discussed so far, the obtained results are shown in Figure 9 on the right side.

Although only the representation of the mode referred to above as 'mode 2a' is shown here, the results for both modes 2a and 2b are still identified with the same mode shape. Moreover, as can be noticed for the representative case here depicted, but is valid for all three instrumented decks, the estimated damping ratios for the first and second modes are slightly higher than those estimated and reported in the previous section.

At the bottom of the images in Figure 9 (d), (e), and (f) the Modal Assurance Criterion (MAC) can be observed to verify the similarity between the identified modes. As already observed through the MATLAB AOMA code, a substantial similarity is observable between the first and fourth (denoted as Mode 3) modes. Similarly, it is possible to visualise complexity plots, which make it possible to indirectly verify whether a mode is physical or, for example, due to numerical effects or acquisition noise, given its complexity.

Finally, the results in terms of identified frequencies for the different system identification approaches used are reported in Table 2. The analysis carried out on the signals of the three spans using commercial software ARTeMIS, using the FDD and SSI-UPC techniques and considering the first three modes, indicates a good correlation in terms of natural frequencies, while a discrepancy is noted in the estimation of modal damping, which on average is higher in ARTeMIS than in the MATLAB code. However, this parameter is known to be the most uncertain of those to be estimated [17] and, for this very reason, is generally not considered in terms of structural monitoring. Given the low standard deviation values, the same conclusions as in Section 4.1 can be replicated here.

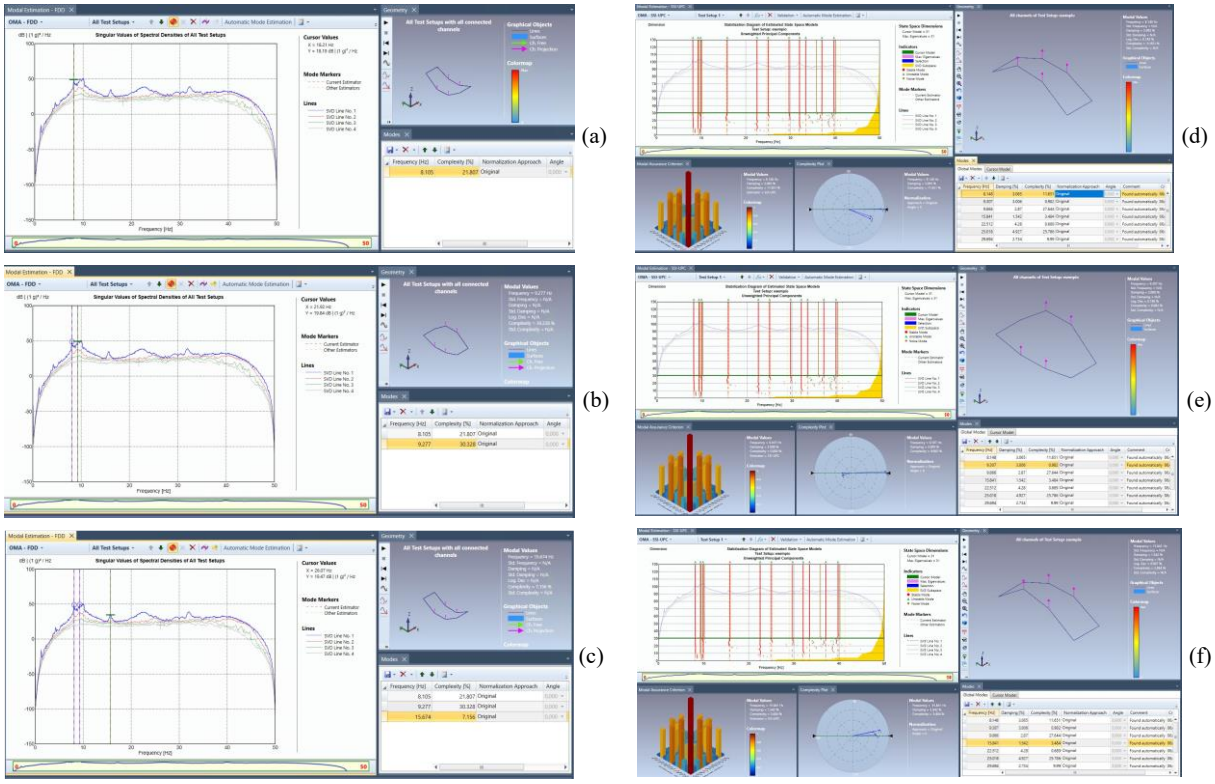

Figure 9: Results obtained in ARTeMIS by applying the FDD method on the left, reporting mode 1 (a), mode 2 (b) and mode 3 (c) manually selected from the signals PSD; and by applying SSI-UPC on the right, showing mode 1 (d), mode 2a (e) and mode 3 (f) estimated automatically.

DOI: 10.3217/978-3-99161-057-1-140

Table 2: Summary of the natural frequencies identified by ARTeMIS (all values in Hz) for the relevant modes in the three instrumented spans with the FDD and SSI-UPC methods, with computation of the average and standard deviation values (St.Dev). The sign '-' indicates unidentified modes.

		Mode 1	Mode 2a	Mode 2b	Mode 3
FDD	Span 1	8.562	9.684	-	15.789
	Span 2	8.255	9.365	10.101	16.034
	Span 3	8.297	-	10.108	16.219
	Average	**8.371**	**9.524**	**10.104**	**16.014**
	St.Dev	**0.166**	**0.226**	**0.005**	**0.216**
SSI-UPC	Span 1	8.461	9.631	10.030	15.777
	Span 2	8.171	9.168	10.197	16.092
	Span 3	8.125	9.231	10.320	16.217
	Average	**8.252**	**9.343**	**10.182**	**16.029**
	St.Dev	**0.182**	**0.251**	**0.145**	**0.227**

Finally, the mode shapes identified in Section 4.1 through the AOMA algorithm developed in MATLAB and those obtained with the two methods implemented in ARTeMIS, as in the present Section, are compared based on Modal Assurance Criterion (MAC), defined as [18]:

$$MAC(\Phi_j, \Phi_k) = \frac{\left[(\Phi_j) * (\Phi_k)\right]^2}{\left[(\Phi_j) * (\Phi_j)\right]\left[(\Phi_k) * (\Phi_k)\right]} \quad (1)$$

The MAC correlation matrices for the instrumented span 1 are summarised in Table 3. The top part of the table shows the MAC values computed between the MATLAB-identified mode shapes and those obtained via the ARTeMIS SSI-UPC method, while the bottom section reports the MAC values with the FDD method. For the other couple spans the results are consistent with those presented.
The resulting MAC values for the modes indicated as 1, 2a, and 3 are reported, with the values of interest highlighted. Such values indicate a high correlation between the two sets of mode shapes.

Table 3: MAC correlation matrices of mode shapes identified for span 1 computed between MATLAB code vs ARTeMIS SSI-UPC (top part) and MATLAB vs ARTeMIS FDD (bottom part).

		MATLAB AOMA		
		Mode 1	Mode 2a	Mode 3
ARTeMIS SSI	Mode 1	0.9948	0.0202	0.9846
	Mode 2a	0.0455	0.9980	0.0046
	Mode 3	0.9667	0.0001	0.9958
ARTeMIS FDD	Mode 1	0.9846	4.44e-05	0.9882
	Mode 2a	0.0031	0.9697	0.0044
	Mode 3	0.9974	0.0189	0.9971

The results suggest that the modes obtained from the SSI-UPC automated method present excellent comparability with those obtained in MATLAB, showing a better reliability with respect to the FDD identifications.
It is noteworthy to notice the high MAC values between modes 1 and 3 in both cases, as expected by the nature of the mode shapes (see Figure 8 and Figure 9).

4.3 Effects of train passages

The dynamic data recording included train transit events, presenting signals with much higher acceleration amplitudes but extremely short durations. The analysis of such portions of signals could be of particular interest in the case where less performing accelerometers are used, and as a consequence, are not able to detect vibrations due to environmental excitation, or in the case where load tests need to be performed on the structure, since in such loading conditions the identified modal parameters are in general more sensitive to longitudinal prestressing losses. These signals, if taken in their entirety (i.e. including train passages), become non-stationary and, therefore, difficult to analyse with algorithms intended for stationary analysis, such as SSI. For this reason, if one wants to exploit the excitation given by the passage of trains to extract damage-sensitive modal parameters, it is necessary to resort to other algorithms designed for modal identification and exploiting the excitation contained in the free vibration following a train passage. This aspect will be further explored as part of future developments of this project.

5 CONCLUSIONS

The primary aim of this study was to evaluate the applicability of a novel Automated Operational Modal Analysis (AOMA) algorithm for continuous Structural Health Monitoring (SHM) of a railway bridge. Three spans of this case study were instrumented with high-performance accelerometers. The workflow followed here, from the pre-processing phase of the ambient vibration measurements data to the Automated OMA, made it possible to identify natural frequencies, damping ratios, and mode shapes for the first relevant modes in the frequency range from 0 to 20 Hz, discarding spurious identifications.

The comparison between the AOMA algorithm developed in the MATLAB environment and the commercial software ARTeMIS shows that both approaches provide consistent and reliable results. The similarity in outcomes confirms the validity and robustness of the proposed method, ensuring its applicability. Since the bridge spans are nominally identical, the approach followed for this research study enables the estimation of the variability of the results under the same analysis methodology.

Overall, in view of a broader approach to infrastructure monitoring, maintenance, and management, these findings validate the feasibility of using AOMA for continuous SHM of railway bridges and damage detection.

ACKNOWLEDGMENTS

The study presented here was carried out as part of the program of activities carried out within the MOST – Sustainable Mobility National Research Center and received funding from the European Union Next-GenerationEU

DOI: 10.3217/978-3-99161-057-1-140

(PIANO NAZIONALE DI RIPRESA E RESILIENZA (PNRR) – MISSIONE 4 COMPONENTE 2, INVESTIMENTO 1.4 – D.D. 1033 17/06/2022).

REFERENCES

[1] B. Paulsson, J. Olofsson, H. Hedlund, B. Bell, B. Täljsten, and L. Elfgren, "Sustainable Bridges–Results from a European Integrated Research Project," in *Proceedings of the IABSE Symposium Report*, International Association for Bridge and Structural Engineering: Zurich, Switzerland, 2010, pp. 17–24.

[2] F. Biondini *et al.*, "BRIDGE|50 research project: Residual structural performance of a 50-year-old bridge," *Bridge Maintenance, Safety, Management, Life-Cycle Sustainability and Innovations - Proceedings of the 10th International Conference on Bridge Maintenance, Safety and Management, IABMAS 2020*, pp. 3337–3344, Apr. 2021, doi: 10.1201/9780429279119-453.

[3] M. D'Angelo *et al.*, "Bridge Collapses in Italy across the 21st Century: Survey and Statistical Analysis," *Structure and Infrastructure Engineering (Accepted for publication)*, 2025.

[4] C. R. Farrar and K. Worden, *Structural Health Monitoring: A Machine Learning Perspective*. 2013.

[5] M. P. Limongelli, "Frequency response function interpolation for damage detection under changing environment," *Mech Syst Signal Process*, vol. 24, no. 8, pp. 2898–2913, Nov. 2010, doi: 10.1016/J.YMSSP.2010.03.004.

[6] D. Martucci, M. Civera, and C. Surace, "Bridge monitoring: Application of the extreme function theory for damage detection on the I-40 case study," *Eng Struct*, vol. 279, p. 115573, Mar. 2023, doi: 10.1016/J.ENGSTRUCT.2022.115573.

[7] P. Van Overschee and B. De Moor, *Subspace Identification for Linear Systems*. Boston, MA: Springer US, 1996. doi: 10.1007/978-1-4613-0465-4.

[8] C. Rainieri and G. Fabbrocino, *Operational Modal Analysis of Civil Engineering Structures*. New York, NY: Springer New York, 2014. doi: 10.1007/978-1-4939-0767-0.

[9] E. Reynders, J. Houbrechts, and G. De Roeck, "Fully automated (operational) modal analysis," *Mech Syst Signal Process*, vol. 29, pp. 228–250, May 2012, doi: 10.1016/j.ymssp.2012.01.007.

[10] F. Magalhães, Á. Cunha, and E. Caetano, "Online automatic identification of the modal parameters of a long span arch bridge," *Mech Syst Signal Process*, vol. 23, no. 2, pp. 316–329, Feb. 2009, doi: 10.1016/j.ymssp.2008.05.003.

[11] C. Rainieri and G. Fabbrocino, "Development and validation of an automated operational modal analysis algorithm for vibration-based monitoring and tensile load estimation," *Mech Syst Signal Process*, vol. 60–61, pp. 512–534, Aug. 2015, doi: 10.1016/j.ymssp.2015.01.019.

[12] F. Ubertini, C. Gentile, and A. L. Materazzi, "Automated modal identification in operational conditions and its application to bridges," *Eng Struct*, vol. 46, pp. 264–278, Jan. 2013, doi: 10.1016/j.engstruct.2012.07.031.

[13] M. Civera, L. Sibille, L. Zanotti Fragonara, and R. Ceravolo, "A DBSCAN-based automated operational modal analysis algorithm for bridge monitoring," *Measurement*, vol. 208, p. 112451, Feb. 2023, doi: 10.1016/j.measurement.2023.112451.

[14] M. Ester, H.-P. Kriegel, J. Sander, and X. Xu, "A density-based algorithm for discovering clusters in large spatial databases with noise," in *Proceedings of the Second International Conference on Knowledge Discovery and Data Mining*, 1996, pp. 226–231.

[15] V. Mugnaini, L. Zanotti Fragonara, and M. Civera, "A machine learning approach for automatic operational modal analysis," *Mech Syst Signal Process*, vol. 170, p. 108813, May 2022, doi: 10.1016/j.ymssp.2022.108813.

[16] L. A. Bull *et al.*, "Foundations of population-based SHM, Part I: Homogeneous populations and forms," *Mech Syst Signal Process*, vol. 148, p. 107141, Feb. 2021, doi: 10.1016/j.ymssp.2020.107141.

[17] E. Reynders, R. Pintelon, and G. De Roeck, "Uncertainty bounds on modal parameters obtained from stochastic subspace identification," *Mech Syst Signal Process*, vol. 22, no. 4, pp. 948–969, May 2008, doi: 10.1016/j.ymssp.2007.10.009.

[18] R. Allemang and David. L. Brown, "A Correlation Coefficient for Modal Vector Analysis," in *Proc. 1st Int. Modal Analysis Conference*, 1982.